Determination of the Atropisomeric Stability and Solution Conformation of Asymmetrically Substituted Biphenyls by Means of Vibrational Circular Dichroism (VCD)

by **Teresa B. Freedman***[a]), **Xiaolin Cao**[a]), **Laurence A. Nafie***[a]), **Monica Kalbermatter**[b]), **Anthony Linden**[b]), and **Andreas Johannes Rippert***[b])[1])

[a]) Department of Chemistry, 1-014 Center for Science and Technology, Syracuse University, Syracuse, NY 13244-4100, USA

[b]) Organisch-Chemisches Institut der Universität Zürich, Winterthurerstr. 190, CH-8057 Zurich

Vibrational-circular-dichroism (VCD) studies of the solution conformations of three 2,2′-substituted biphenyls are reported. Biphenyls with only two substituents at the *peri*-position normally show rotation about their central axis of chirality at room temperature in solution. We previously found no evidence for rotation of (*P*,4*S*)-2-[4,5-dihydro-4-(1-methylethyl)oxazol-2-yl]-2′-(hydroxymethyl)-1,1′-biphenyl (**1**) in $CDCl_3$ about its 1,1′- axis, due to stabilization by intramolecular H-bonding and the presence of the i-Pr substituent, but two conformers were found in solution that result from rotation of the heterocycle in **1** between OH ··· N (the form present in the solid state) and the OH ··· O H-bonded forms, with no rotation of the i-Pr group or (*P*) → (*M*) twist [1]. For (*P*,*S*)-**2**, where the i-Pr substituent of **1** has been replaced by a Ph group, rotation of the heterocycle takes place in $CDCl_3$ solution. For (*P*,*S*)-**3** and (*M*,*S*)-**4**, where Me substitution at the two 6,6′-positions of (*P*,*S*)-**1** prevents rotation about the central axis of chirality, rotation of the heterocycle is observed for the (*P*)-configuration ((*P*,*S*)-**3**), but not for the (*M*)-configuration ((*M*,*S*)-**4**). Only one rotamer involving the i-Pr group, which was found in the solid state of (*P*,*S*)-**3**, was also observed in solution, but (*M*,*S*)-**4**, obtained as an oil, was found to be a mixture of three rotamers of the i-Pr group.

1. Introduction. – In a recent study [1] of (*P*,4*S*)-2-[4,5-dihydro-4-(1-methylethyl)-oxazol-2-yl]-2′-(hydroxymethyl)-1,1′-biphenyl (**1**) by vibrational circular dichroism (VCD), we reported an unusual atropisomeric stability, as shown in *Scheme 1*. Biphenyls with only two substituents at the 2,2′-positions normally exhibit rotation about their 1,1′-axes, but, for (*P*,*S*)-**1** in $CDCl_3$ solution in the temperature range 5 to 23°, rotation of the heterocycle (20% **1**-1a, 80% **1**-2a) was observed, with no evidence for (*P*) → (*M*) rotation, and no rotation of the i-Pr group in the rotamer found in the crystal structure. We report here an extension of this work to three additional biphenyls (**2**–**4**) where the i-Pr group of **1** has been replaced by a Ph group (**2**) and where Me substituents at the 6,6′-positions allow resolution of the stable atropisomers (*P*,*S*)-**3** and (*M*,*S*)-**4**.

VCD is a sensitive probe of solution conformation and absolute configuration [2][3]. The technique entails comparison of observed VCD spectra with calculations carried out at the density-functional-theory (DFT) level, and has been applied to a wide variety of samples [2–8]. The fast vibrational timescale allows observation of VCD features corresponding to individual conformers in solution.

---

[1]) Present address: Kantonspolizei Zürich, Urkundenlabor, Postfach, CH-8021 Zürich.

Scheme 1

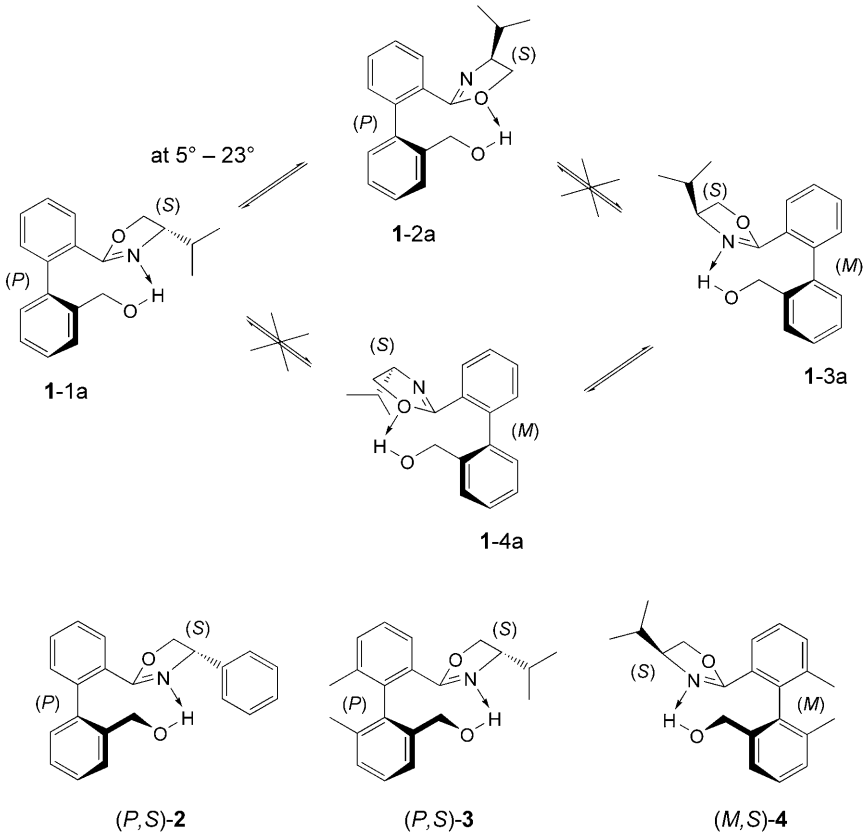

2. Results and Discussion. – Compounds **1** – **4** were synthesized in a straightforward manner, and the synthetic and spectroscopic details will be published in a subsequent paper [9]. These compounds are of great importance for us, as they result from our synthetic efforts to build up a variety of suitable ligands for transition metal catalyzed reactions. The solid-state structures found by X-ray crystallographic analyses of (*P*,*S*)-**2** and (*P*,*S*)-**3** are presented in *Fig. 1*; they are analogous to that of (*P*,*S*)-**1** [1].

As in the case of (*P*,*S*)-**1**, the crystals contained enantiomerically and diastereoisomerically pure (*P*,*S*)-**2** and (*P*,*S*)-**3**. For (*P*,*S*)-**2**, where (*S*)-phenylglycine had been used as the enantiomerically pure amino alcohol, the two diastereoisomers (*P*,*S*)- and (*M*,*S*)-**2** can be expected. However, as these diastereoisomers have only two 2,2′-substituents, they should be in equilibrium in solution at room temperature. In contrast, compound (*P*,*S*)-**3** has additional Me substituents at the 6,6′-positions, and no rotation about the central axis of chirality can take place. Therefore, diastereoisomers are formed and can be separated.

The H-bonding patterns that were found for (*P*,*S*)-**2** and (*P*,*S*)-**3** were very similar to that in (*P*,*S*)-**1** [1], as well as the almost perpendicular arrangement of the two Ph rings of the biphenyl backbone (*Table 1*).

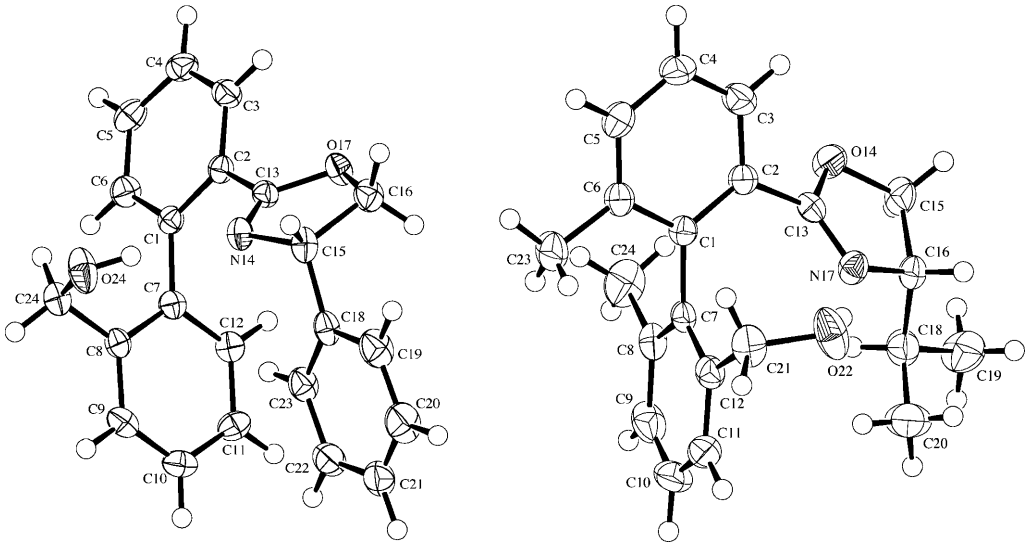

Fig. 1. *X-Ray crystal structures of (*P,S*)*-**2** (left) *and (*P,S*)*-**3** (right). ORTEP Representation at the 50% probability level; arbitrary atom numbering.

Table 1. *H-Bonding Parameters* (OH···N) *and Biphenyl Twist Angles in (*P,S*)*-**1**, *(*P,S*)*-**2**, *and (*P,S*)*-**3**

Compound	H···N [Å]	O···N [Å]	OH···N angle [°]	Biphenyl angle [°]
(*P,S*)-**1**[a])	1.87(2)	2.845(2)	175(2)	89.00(8)
(*P,S*)-**2**	1.96(2)	2.841(1)	174(1)	81.48(6)
(*P,S*)-**3**	1.91(3)	2.871(2)	169(2)	84.65(8)

[a]) Data taken from [1].

Furthermore, an additional small stabilizing effect was visible for the observed conformation in these two new structures, namely the substituent on the dihydrooxazole ring, *i.e.*, the Ph or the i-Pr group, resides over the plane of one of the benzene rings of the biphenyl moiety, which is indicative of the presence of CH···π interactions (*Table 2*). However, this interaction is weak and, therefore, in solution, the activation energy for the rotation of the i-Pr group in compounds (*P,S*)-**1** and (*P,S*)-**3** is expected to be small, and will not vary much from that in alkane chains. In compound (*P,S*)-**2**,

Table 2. *CH···π Interactions between the 4-Substituent of the Dihydrooxazole Ring and the Counter Benzene Rings of the Biphenyl Moiety in (*P,S*)*-**1**, *(*P,S*)*-**2**, *and (*P,S*)*-**3**

Compound	Distance H···Ph (centroid) [Å]	Angle H···Ph (centroid) [°]
(*P,S*)-**1**[a])	3.18	165
(*P,S*)-**2**	2.54	162
(*P,S*)-**3**	3.27	156

[a]) Data taken from [1].

which carries a Ph substituent at the dihydrooxazole ring, the CH$\cdots\pi$ distance is with 2.54 Å significantly shorter than in the other two structures (3.18–3.27 Å; *Table 2*). The shorter distance allows for a perfect edge-to-face arrangement, which is mainly favored by the geometric arrangement of the biphenyl unit and the side chain to allow an interaction between two acceptors, with a H-atom in between, namely one Ph ring of the biphenyl moiety as a π-acceptor, and the Ph ring of the side chain as a σ-acceptor [10].

To determine whether the rotation of the heterocycle in (*P*,*S*)-**1**, without any rotation about the axis of chirality, is also the case for other substitution patterns in this class of compounds, and to show that VCD measurements are a valuable tool for gaining deeper insight into the conformational arrangements of molecules in solution, we carried out detailed VCD measurements in $CDCl_3$ for (*P*,*S*)-**2**, (*P*,*S*)-**3** and (*M*,*S*)-**4**. Their IR and VCD spectra in $CDCl_3$ are presented in *Fig. 2*. An overlay of the spectra of the diastereoisomers (*P*,*S*)-**3** and (*M*,*S*)-**4** (*Fig. 3*,*a*), reveals several regions with approximate mirror-image VCD features that are indicative of the atropisomers, and features of the same sign near 1350 cm^{-1} associated with vibrations of groups at the common (*S*)-configured center of the dihydrooxazole ring. The overall VCD intensity for **2** was smaller by a factor of *ca.* 2 compared to those of **3** and **4**. A comparison of the IR and VCD spectra for (*P*,*S*)-**1** and (*P*,*S*)-**2** in $CDCl_3$ solution is presented in *Fig. 3*,*b*.

Calculations for biphenyl (*S*)-**2**, gave rise to four optimized conformers (*Fig. 4*), with calculated relative energies for the isolated (*P*)- or (*M*)-twist species and rotation of the dihydrooxazole group to permit either OH$\cdots$N or OH$\cdots$O H-bonding. We found only one stable orientation of the Ph substituent of the dihydrooxazole moiety. For the gas-phase species at this level of calculation, OH$\cdots$N H-bonding was calculated to be much stronger than OH$\cdots$O H-bonding. However, the experimental data suggested much smaller differences in energy for these types of interactions in solution species. A comparison of the calculated IR and VCD spectra for the four conformers with the observed spectra obtained by dissolving the crystalline compound with conformation **2**-PN, shown in *Fig. 5*,*a*, revealed features in the observed VCD spectrum that correlate with bands for each of the two (*P*)-twist conformers, but no observed features unique only to the (*M*)-twist conformers. Good agreement with the observed VCD spectrum was obtained for a **2**-PN/**2**-PO 80:20 composite (*Fig. 5*,*a*). The composite spectrum with 80% (*P*)-twist and 20% (*M*)-twist, both with a 4:1 ratio of dihydrooxazole rotamers, yielded a similar fit, with a slight decrease in the intensity of VCD features 2, 3, 4 and 9 (*cf. Fig. 5*,*b*).

In contrast to biphenyl **1** with an i-Pr substituent, for which the differences in the calculated spectra for the two atropisomers were more distinct and no evidence for (*P*) $\rightarrow$ (*M*) conversion was observed, a small solution population of (*M*)-twist cannot be ruled out for the Ph-substituted **2**. However, the similarity in overall VCD intensity for solutions of (*P*,*S*)-**1** and (*P*,*S*)-**2**, shown in *Fig. 3*,*b* suggests atropisomeric stability for both compounds in $CDCl_3$ solution, since admixture of the (*M*)-twist conformers decreases the overall VCD intensity.

For biphenyls (*P*,*S*)-**3** and (*M*,*S*)-**4**, the Me groups in 6- and 6′-position prohibit rotation about the central 1,1′-axis. Biphenyl (*P*,*S*)-**3** was obtained as a crystalline compound with a single i-Pr rotamer, and with OH$\cdots$N H-bonding. Six solution

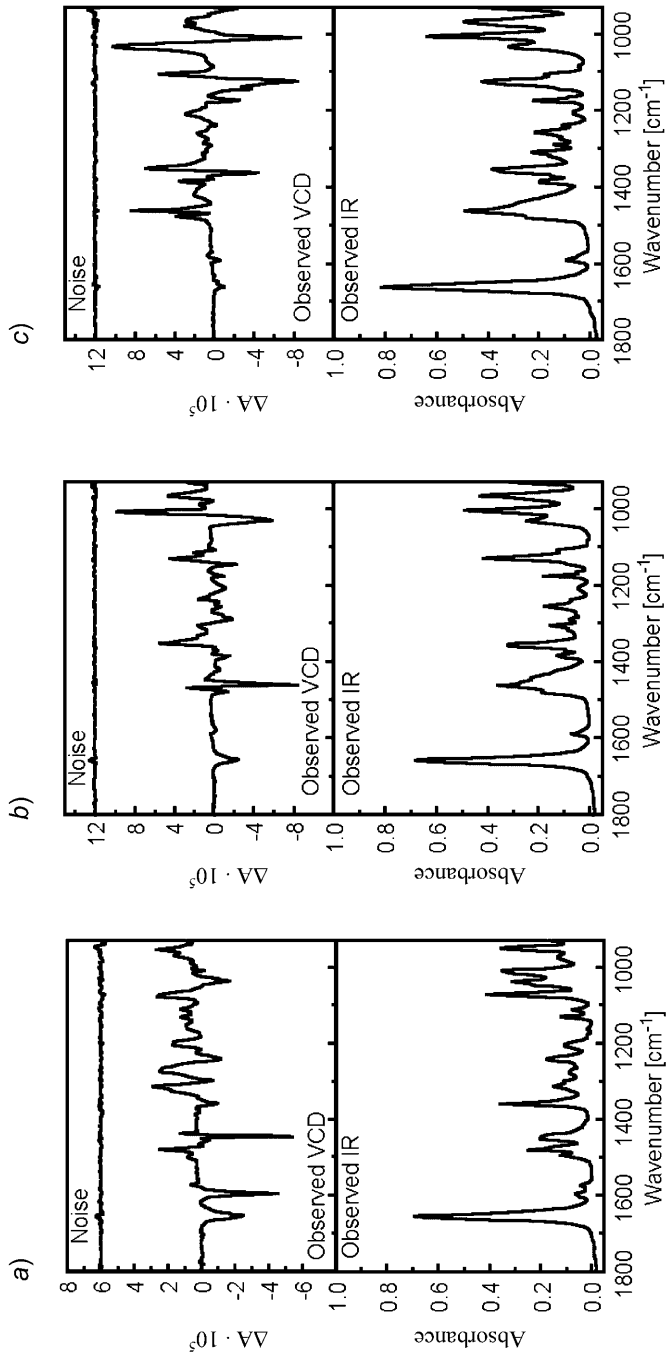

Fig. 2. *Observed IR* (lower frames) *and VCD* (upper frames) *spectra of* a) (*P*,*S*)-**2**, b) (*P*,*S*)-**3**, *and* c) (*M*,*S*)-**4** *in* $CDCl_3$ *solution*. Conditions: 23°, BaF_2 cell (98 μm), data collection over 9 h at 4 cm^{-1} resolution, optimized at 1400 cm^{-1}. Uppermost traces are the VCD noise.

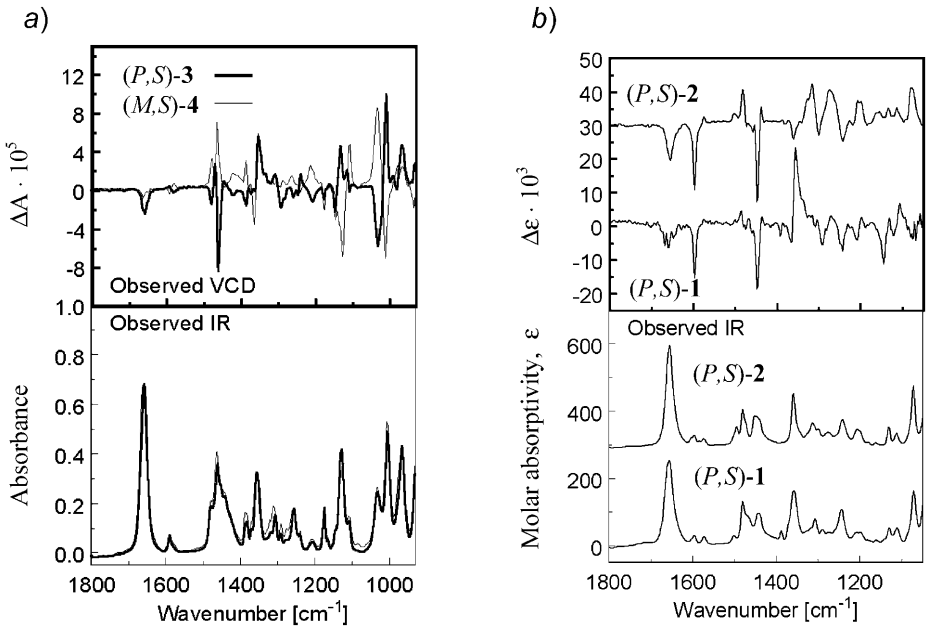

Fig. 3. a) *Overlay of the IR* (lower frame) *and VCD* (upper frame) *spectra for (*P,S*)-**3** and (*M,S*)-**4**.* b) *Comparison of the VCD* (upper frame) *and IR* (lower frame) *spectra of (*P,S*)-**1** and (*P,S*)-**2** in $CDCl_3$ solution.*

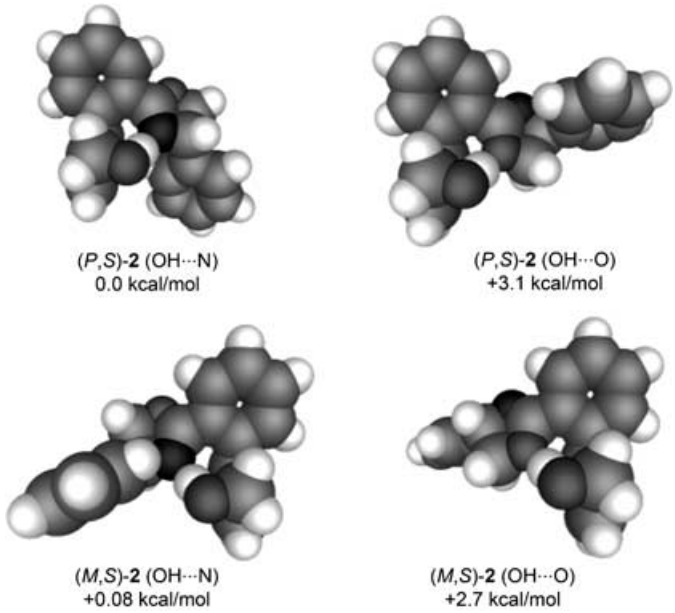

Fig. 4. *Structures and relative energies of the optimized conformers of (*S*)-**2**, with (*P*)- or (*M*)-helical twist, and OH···N or OH···O H-bonding*

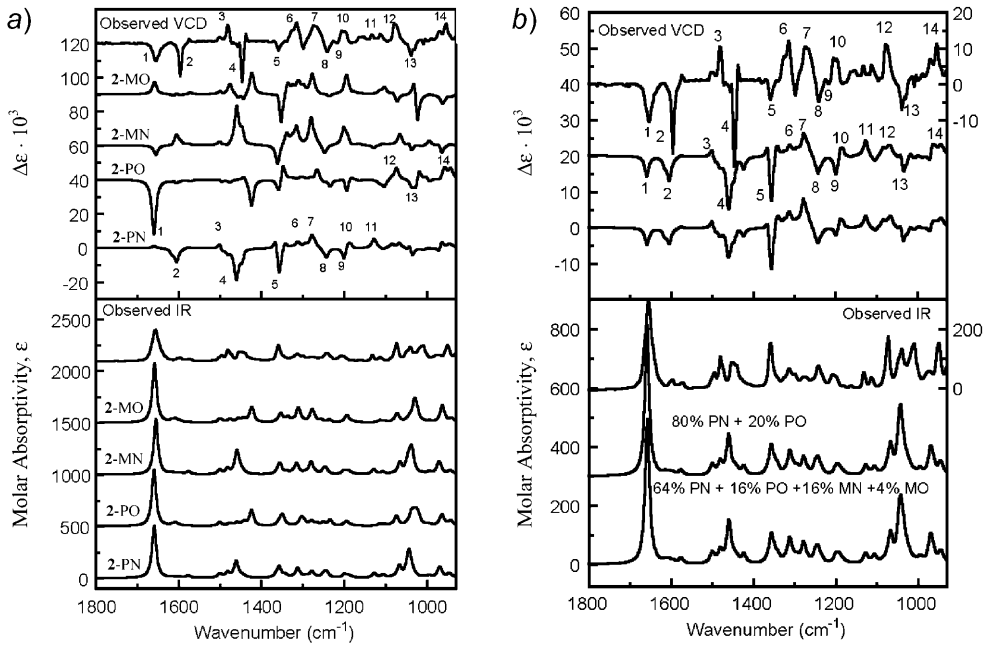

Fig. 5. a) *IR* (lower frame) *and VCD* (upper frame) *spectra calculated* (left axes) *for four conformers of* (P,S)-**2** *compared with the observed spectra* (right axes). Numbers identify correlations for VCD bands; spectra offset for clarity. b) *Comparison of the observed IR and VCD spectra of* (P,S)-**2** (upper traces, right axes) *with composite-calculated spectra* (left axes) *for* **2**-*PN*/**2**-*PO 80:20* (center traces) *and for* **2**-*PN*/**2**-*PO*/**2**-*MN*/**2**-*MO 64:16:16:4* (lower traces).

conformations are possible, with three rotamers of the i-Pr group, and rotation of the dihydrooxazole moiety. Comparison of observed $CDCl_3$ solution VCD spectra of **3** with calculated spectra for two dihydrooxazole conformers (*Fig. 6*, each with the i-Pr orientation found in the crystal) are shown in *Fig. 7,a*. Correlation between the observed and calculated features provides evidence for both H-bonded rotamers. In this case, the best agreement in sign and relative intensity between observed and

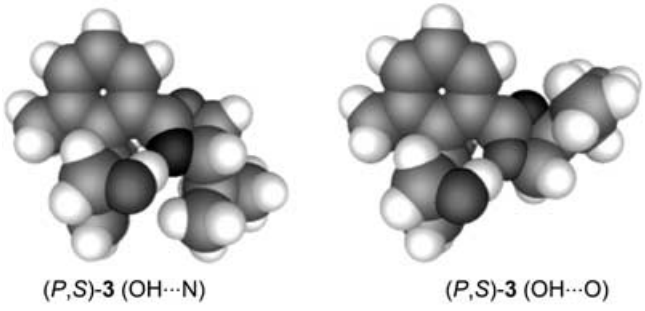

Fig. 6. *Calculated optimal geometries for* (P,S)-**3** *with crystal orientation of the isopropyl group*

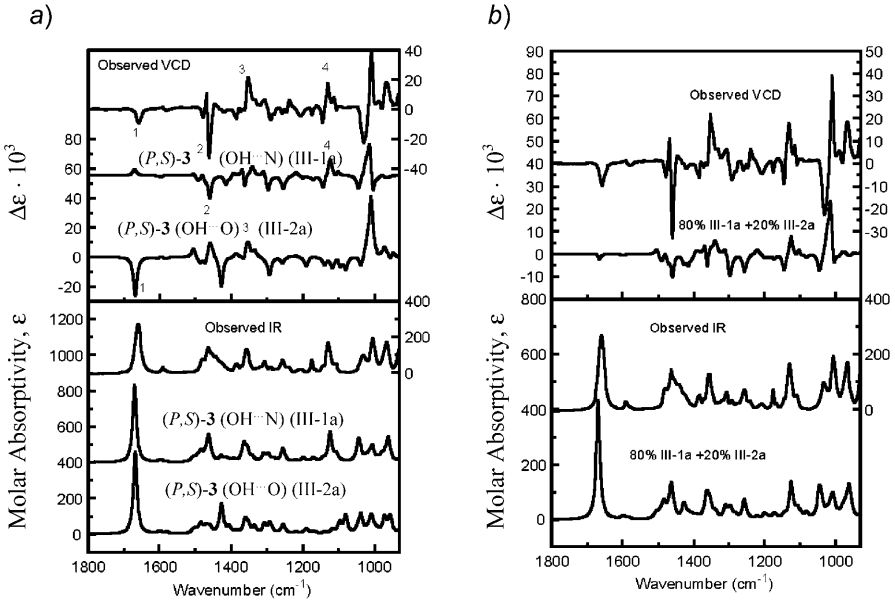

Fig. 7. a) *IR* (lower frame) *and VCD* (upper frame) *spectra calculated for two conformers of* (P,S)-**3**. Numbers identify correlations for VCD bands; spectra offset for clarity. b) *Comparison of the observed IR and VCD spectra of* (P,S)-**3** (upper traces, right axes) *with composite-calculated spectra for 80%* (P,S)-**3** *(OH···N; III-1a) plus 20%* (P,S)-**3** *(OH···O; III-2a)* (lower traces, left axes).

calculated spectra was obtained for 80% (*P*,*S*)-**3** (OH···N) (III-1a) and 20% (*P*,*S*)-**3** (OH···O) (III-2a) (*Fig. 7*,*b*). Distinct features characteristic of other i-Pr rotamers are not identified in the calculated spectra, and an admixture of calculated spectra for the other rotamers (not shown) degrades the fit with the observed data shown in *Fig. 7*,*b*.

For (*P*,*S*)-**4**, the calculated spectra for all three i-Pr rotamers (*Fig. 8*) with OH···N H-bonding and one rotamer with OH···O H-bonding, are compared with the observed spectra in *Fig. 9*,*a*. No distinct features corresponding to OH···O H-bonded forms were found in the observed spectra. All three i-Pr group rotamers with OH···O H-bonding exhibit intense positive VCD near 1660 cm^{-1}, in contrast to the weak VCD at this frequency for all OH···N conformers, and to the weak negative VCD observed at this frequency. The best fit to calculation is found for equal populations of the three i-Pr group rotamers with OH···N H-bonding, as shown in *Fig. 9*,*b*. In this case, the fit to the negative VCD feature at 1125 cm^{-1} requires a population (33%) of (*M*,*S*)-**4** (OH···N; IV-3c) above that predicted (10%) from the relative energies calculated for the isolated molecules. In contrast to **1** and **3**, which were present as crystalline samples and for which only the crystal conformation of the i-Pr group was found for the corresponding $CDCl_3$ solutions, (*M*,*S*)-**4** was obtained as an oil, and the VCD spectra indicated a mixture of i-Pr group rotamers. Although the presence of small populations of OH···O rotamers cannot be ruled out from the VCD analysis, introducing an OH···N/OH···O 80:20 mixture for the three i-Pr group rotamers with an (*M*)-configuration

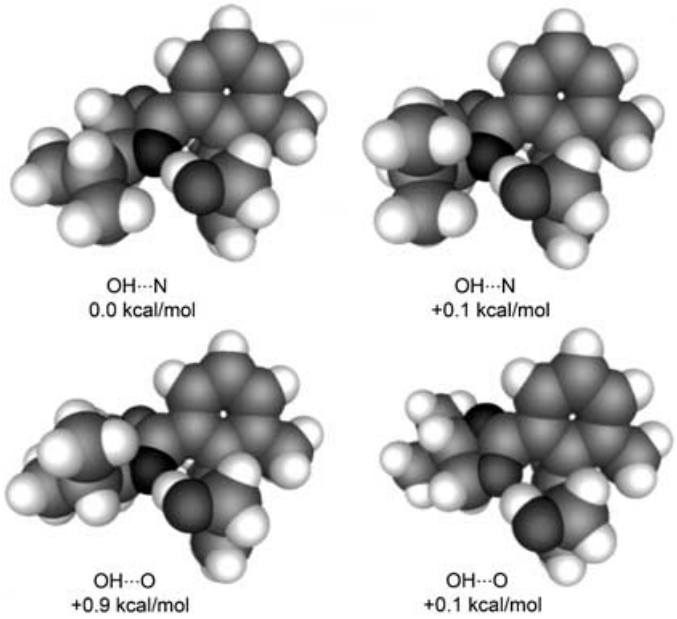

Fig. 8. *Calculated optimal geometries and relative energies for three isopropyl group rotamers of (*M,S*)-***4*** with OH···N H-bonding, and one rotamer with OH···O H-bonding*

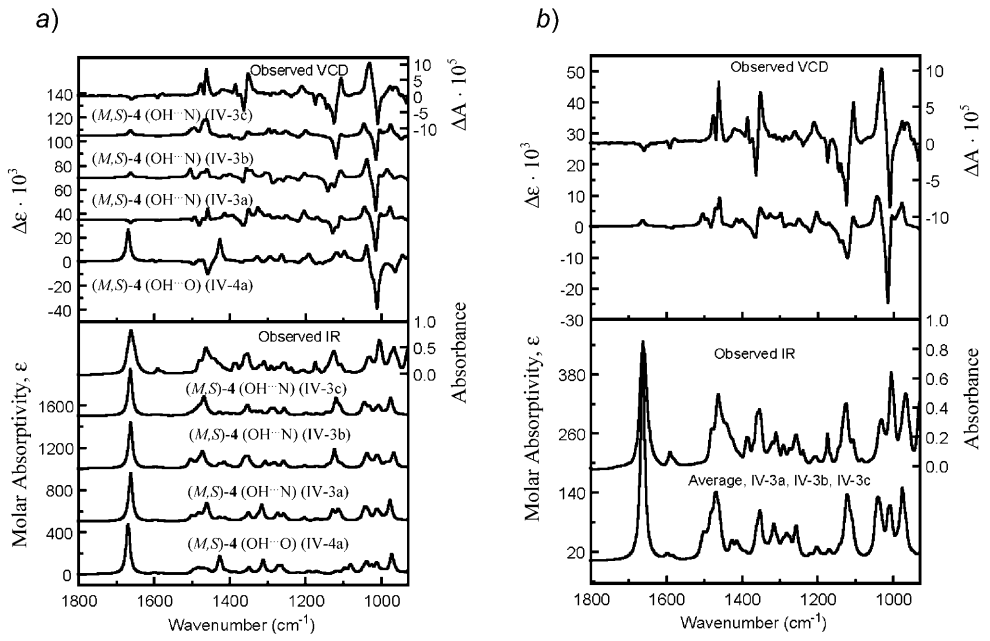

Fig. 9. a) *IR* (lower frame) *and VCD* (upper frame) *spectra calculated* (left axes) *for four conformers of (*M,S*)-***4*** compared with the observed spectra* (right axes). Numbers identify correlations for VCD bands; spectra offset for clarity. b) *Comparison of the observed IR and VCD spectra of (*M,S*)-***4*** (upper traces, right axes) with composite-calculated spectra for an average of conformers IV-1a, IV-1b and IV-1c* (lower traces, left axes).

(comparable with that found for the single i-Pr group rotamer for (*P,S*)-**3**), results in a distinct positive VCD feature at *ca.* 1660 cm^{-1}, and lower intensities for most of the remaining VCD bands, which degrades the overall fit.

3. Conclusions. – The results of this VCD investigation of the solution conformations of three asymmetrically substituted biphenyls are summarized in *Scheme 2*. For

Scheme 2

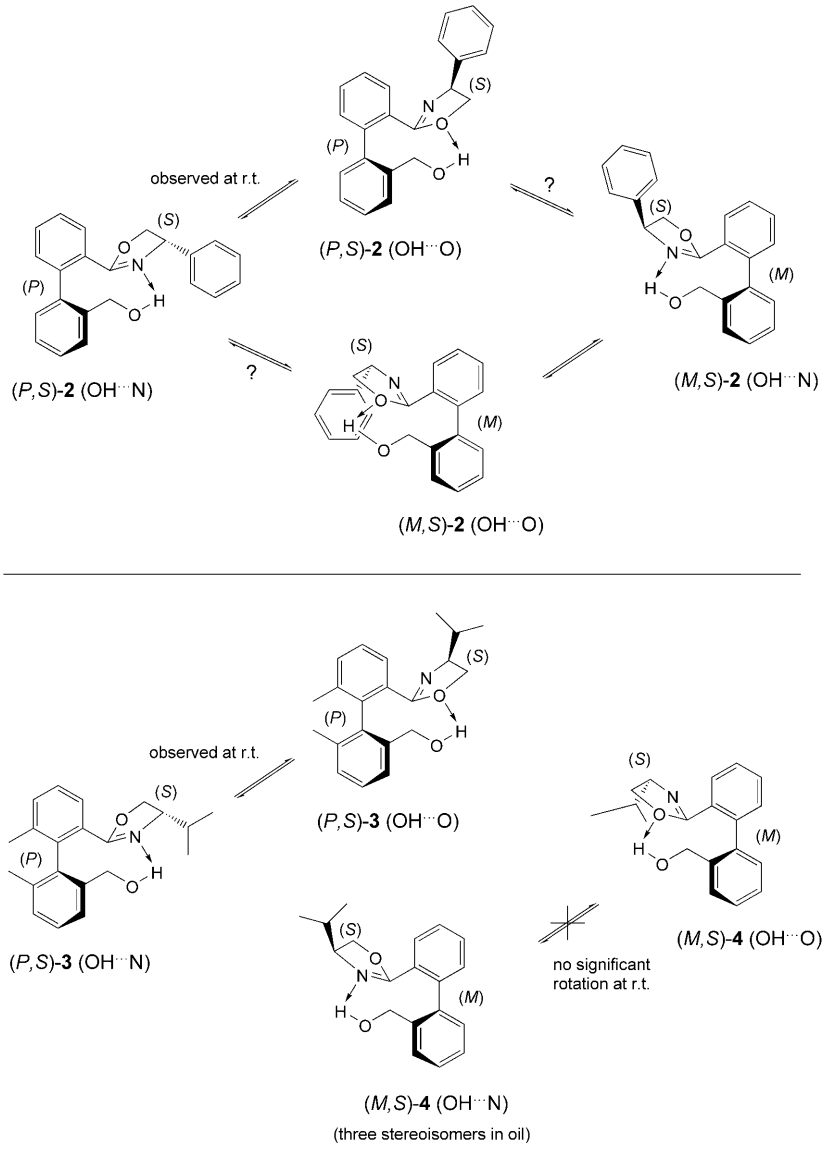

(*P*,*S*)-**2**, dissolving the single OH···N H-bonded rotamer in $CDCl_3$ results in an equilibrium between the two dihydrooxazole rotamers, as also found previously for (*P*,*S*)-**1**. The VCD spectra are consistent with the atropisomeric stability for (*P*,*S*)-**2**, but small amounts of (*M*,*S*)-**2** cannot be ruled out from this study. For (*P*,*S*)-**3**, an equilibrium between OH···N and OH···O rotamers is also established, with no rotation of the i-Pr group rotamer, as found in the crystal orientation. For (*M*,*S*)-**4**, obtained as an oil, the VCD spectra in $CDCl_3$ solution are consistent with the presence of three i-Pr group rotamers with OH···N H-bonding, but the lack of OH···O H-bonded conformers.

Experimental Part

General. Compounds **2**–**4** were prepared in analogy to **1** [1], and the exper. details will be published in a subsequent paper [9]. All IR and VCD spectra were recorded on a modified 'Chirali*r*' VCD spectrometer (*BioTools*, Inc.) at 4 cm^{-1} resolution, 9-h collection for sample and solvent, with the instrument optimized at 1400 cm^{-1}. The IR and VCD spectra were obtained for solutions in $CDCl_3$ solvent (10.3 mg/130 µl $CDCl_3$ for (*P*,*S*)-**2**, 10.1 mg/120 µl $CDCl_3$ for (*P*,*S*)-**3**, and an unknown concentration for (*M*,*S*)-**4** (oil)) in a 98-µm-path length BaF_2 cell at r.t.

Calculations. Conformers for (*S*)-**2**, (*S*)-**3**, and (*S*)-**4** were modeled with the HyperChem software (*Hypercube*, *Inc.*, Gainesville, FL), and the geometries were optimized with Gaussian 98 [11] at DFT level, with the B3LYP functional and the 6-31G(d) basis set. The vibrational frequencies and IR and VCD intensities were calculated with Gaussian 98 at the same DFT level, with the magnetic-field-perturbation method [12] for VCD incorporated into Gaussian 98 based on gauge-invariant atomic orbitals [13][14]. The frequencies were scaled by a factor of 0.97, and the intensities were converted to *Lorentzian* bands with a half-width of 4-cm^{-1} for comparison with the experimental data.

X-Ray Crystal-Structure Determination of (P,S)-**2** *and* (P,S)-**3** (see *Table 3 and Fig. 1*[2])). All measurements were conducted on a *Nonius KappaCCD* area-detector diffractometer [15] using graphite-monochromated MoK_α radiation (λ 0.71073 Å) and an *Oxford Cryosystems Cryostream-700* cooler. Data reduction was performed with HKL Denzo and Scalepack [16]. The intensities were corrected for *Lorentz* and polarization effects, but not for absorption. Equivalent reflections, other than *Friedel* pairs, were merged. The data collection and refinement parameters are given in *Table 3*, and views of the molecules are shown in *Fig. 1*. The structures were solved by direct methods [17]. The non-H-atoms were refined anisotropically. In each case, the OH H-atom was placed in the position indicated by a difference-electron-density map, and its position was allowed to refine together with an isotropic displacement parameter. All remaining H-atoms were fixed in geometrically calculated positions (d(C–H) 0.95 Å), and each was assigned a fixed isotropic displacement parameter, with a value equal to 1.2 U_{eq} of its parent C-atom. The absolute configuration could not be determined crystallographically due to the absence of significant anomalous scattering elements in each compound. Instead, the enantiomer used in the refinement was based on the known (*S*)-configuration of the stereogenic center in the oxazole moiety. The refinement of each structure was carried out on F using full-matrix least-squares procedures, which minimized the function $\Sigma w(|F_o| - |F_c|)^2$, where $w = [\sigma^2(F_o) + (0.005F_o)^2]^{-1}$. A correction for secondary extinction was applied. Neutral-atom scattering factors for non-H-atoms were taken from [18a], and the scattering factors for H-atoms from [19]. Anomalous dispersion effects were included in F_c [20]; the values for f' and f''were those of [18b], and the values of the mass attenuation coefficients were those of [18c]. All calculations were performed with the teXsan crystallographic software package [21], and *Fig. 1* was drawn with ORTEP II [22].

---

[2]) CCDC-237720 and CCDC-237721 contain the supplementary crystallographic data for this paper. These data can be obtained free of charge, *via* www.ccdc.cam.ac.uk/data_request/cif or from the *Cambridge Crystallographic Data Centre*, 12 Union Road, Cambridge CB2 1EZ, UK (fax: + 441223336033; e-mail: data_request@ccdc.cam.ac.uk).

Table 3. *Crystallographic Data of Compounds (*P,S*)-***2** *and (*P,S*)-***3**

Crystallized from	^{t}BuOMe	^{t}BuOMe/hexane
Empirical formula	$C_{22}H_{19}NO_2$	$C_{21}H_{25}NO_2$
Formula weight [g mol^{-1}]	329.40	323.43
Crystal color, habit	colorless, prism	colorless, prism
Crystal dimensions [mm]	$0.20 \times 0.25 \times 0.30$	$0.15 \times 0.20 \times 0.25$
Temperature [K]	160(1)	160(1)
Crystal system	orthorhombic	orthorhombic
Space group	$P2_12_12_1$	$P2_12_12_1$
Z	4	4
Reflections for cell determination	2772	2429
2θ Range for cell determination [°]	2 – 60	4 – 55
Unit-cell parameters: a [Å]	7.8233 (1)	8.5982 (1)
b [Å]	12.0705 (2)	10.7573 (2)
c [Å]	17.6492 (2)	19.8707 (3)
V [Å^3]	1666.63 (4)	1837.91 (5)
D_x [g cm^{-3}]	1.313	1.169
$\mu(\mathrm{Mo}K_\alpha)$ [mm^{-1}]	0.0838	0.0743
$2\theta_{max}$ [°]	24469	31077
Symmetry-independent reflections	4848	4216
R_{int}	0.041	0.049
Reflections used [$I > 2\sigma(I)$]	3978	3465
Parameters refined	231	222
Final $R(F)$	0.0425	0.0440
$wR(F)$	0.0349	0.0401
Goodness-of-fit	1.848	2.407
Secondary extinction coefficient	$4.7\ (4) \times 10^{-6}$	$5.1\ (4) \times 10^{-6}$
Final Δ_{max}/σ	0.0003	0.0004
$\Delta\rho$ (max; min) [e Å^{-3}]	0.28; – 0.26	0.22; – 0.25

REFERENCES

[1] T. B. Freedman, X. Cao, L. A. Nafie, M. Kalbermatter, A. Linden, A. J. Rippert, *Helv. Chim. Acta* **2003**, *86*, 3141.

[2] T. B. Freedman, X. Cao, R. K. Dukor, L. A. Nafie, *Chirality* **2003**, *15*, 743.

[3] P. J. Stephens, F. J. Devlin, *Chirality* **2000**, *12*, 172.

[4] A. Solladie-Cavallo, C. Marsol, G. Pescitelli, L. Di Bari, P. Salvadori, X. Huang, N. Fujioka, N. Berova, X. Cao, T. B. Freedman, L. A. Nafie, *Eur. J. Org. Chem.* **2002**, 1788.

[5] T. B. Freedman, X. Cao, R. V. Oliveira, Q. B. Cass, L. A. Nafie, *Chirality* **2003**, *15*, 196.

[6] T. B. Freedman, X. Cao, A. Rajca, H. Wang, L. A. Nafie, *J. Phys. Chem. A* **2003**, *107*, 7692.

[7] B. E. Maryanoff, D. F. McComsey, R. K. Dukor, L. A. Nafie, T. B. Freedman, X. Cao, V. W. Day, *Bioorg. Med. Chem.* **2003**, *11*, 2463.

[8] A. Solladie-Cavallo, C. Marsol, M. Yaakoub, K. Azyat, A. Klein, M. Roje, C. Suteu, T. B. Freedman, X. Cao, L. A. Nafie, *J. Org. Chem.* **2003**, *68*, 7308.

[9] M. Kalbermatter, A. Linden, A. J. Rippert, *Helv. Chim. Acta*, in preparation.

[10] G. R. Desiraju, T. Steiner, 'The Weak Hydrogen Bond in Structural Chemistry and Biology', Oxford University Press, Oxford, 1999, Chapt. 3.

[11] M. J. Frisch, G. W. Trucks, H. B. Schlegel, G. E. Scuseria, M. A. Robb, J. R. Cheeseman, V. G. Zakrzewski, J. A. Montgomery Jr., R. E. Stratmann, J. C. Burant, S. Dapprich, J. M. Millam, A. D. Daniels, K. N. Kudin, M. C. Strain, O. Farkas, J. Tomasi, V. Barone, M. Cossi, R. Cammi, B. Mennucci, C. Pomelli, C. Adamo, S. Clifford, J. Ochterski, G. A. Petersson, P. Y. Ayala, Q. Cui, K. Morokuma, D. K. Malick, A. D. Rabuck, K. Raghavachari, J. B. Foresman, J. Cioslowski, J. V. Ortiz, B. B. Stefanov, G. Liu, A. Liashenko, P. Piskorz, I. Komaromi, R. Gomperts, R. L. Martin, D. J. Fox, T. Keith, M. A. Al-Laham, C. Y. Peng, A. Nanayakkara,

C. Gonzalez, M. Challacombe, P. M. W. Gill, B. Johnson, W. Chen, M. W. Wong, J. L. Andres, C. Gonzalez, M. Head-Gordon, E. S. Replogle, J. A. Pople, Gaussian 98, A.9, *Gaussian, Inc.*, Pittsburgh, PA, 1998

[12] P. J. Stephens, F. J. Devlin, C. F. Chabalowski, M. J. Frisch, *J. Phys. Chem.* **1994**, *98*, 11623.

[13] K. L. Bak, F. J. Devlin, C. S. Ashvar, P. R. Taylor, M. J. Frisch, P. J. Stephens, *J. Phys. Chem.* **1995**, *99*, 14918.

[14] L. A. Nafie, *J. Chem. Phys.* **1992**, *96*, 5687.

[15] R. Hooft, KappaCCD Collect Software, *Nonius BV*, Delft, The Netherlands, 1999.

[16] Z. Otwinowski, W. Minor, *Methods Enzymol.* **1997**, *276*, 307.

[17] G. M. Sheldrick, SHELXS97, Program for the Solution of Crystal Structures, University of Göttingen, Germany, 1997; A. Altomare, G. Cascarano, C. Giacovazzo, A. Guagliardi, M. C. Burla, G. Polidori, M. Camalli, SIR92, *J. Appl. Crystallogr.* **1994**, *27*, 435.

[18] a) E. N. Maslen, A. G. Fox, M. A. O'Keefe, in 'International Tables for Crystallography', Ed. A. J. C. Wilson, Kluwer Academic Publishers, Dordrecht, 1992, Vol. C, Table 6.1.1.1, p. 477; b) D. C. Creagh, W. J. McAuley, in 'International Tables for Crystallography', Ed. A. J. C. Wilson, Kluwer Academic Publishers, Dordrecht, 1992, Vol. C, Table 4.2.6.8, p. 219; c) D. C. Creagh, J. H. Hubbell, in 'International Tables for Crystallography', Ed. A. J. C. Wilson, Kluwer Academic Publishers, Dordrecht, 1992, Vol. C, Table 4.2.4.3, p. 200.

[19] R. F. Stewart, E. R. Davidson, W. T. Simpson, *J. Chem. Phys.* **1965**, *42*, 3175.

[20] J. A. Ibers, W. C. Hamilton, *Acta Crystallogr.* **1964**, *17*, 781.

[21] teXsan: Single Crystal Structure Analysis Software, Version 1.10, *Molecular Structure Corporation*, The Woodlands, TX, 1999.

[22] C. K. Johnson, ORTEPII, Report ORNL-5138, Oak Ridge National Laboratory, Oak Ridge, TN, 1976.

Received January 24, 2005